Journal of Engineering Science and Technology
Vol. 12, No. 4 (2017) 1048 - 1066

COLD FLOW ANALYSIS ON INTERNAL COMBUSTION ENGINE WITH DIFFERENT PISTON BOWL CONFIGURATIONS

N. A. MOHAMAD SHAFIE, M. F. MUHAMAD SAID*

Automotive Development Centre, Faculty of Mechanical Engineering,
Universiti Teknologi Malaysia, 81310, UTM Johor Bahru, Malaysia
*Corresponding Author: mfarid@fkm.utm.my

Abstract

Development of engine in automotive industry is deemed critical in order to fulfil demands by passengers and also due to pressure bring forward by the fact of stringent government law for protecting noise and air quality. In order to improve engine quality, understanding on flow properties in engine cylinder is of major importance because flow condition significantly influences engine efficiency. Capabilities in providing optimum flow conditions which include high discharge coefficient, optimum swirl ratio, and optimum tumble ratio in respective engine can result in enhancement of engine power and comfort, along with reduction of fuel consumption, exhaust emission and noise. This research aims to investigate the effect of different piston bowl configurations on in-cylinder flow characteristics. Cold flow simulation is used to compare in-cylinder flow for engine with three different piston bowls during intake stroke and compression stroke. Simulation analysis represents the flow properties in term of swirl ratio and tumble ratio. Result computed from this analysis shows that piston bowl geometry has little influence on in-cylinder flow during intake stroke. However, piston bowls configurations inflicted significant effect on flow during compression stroke especially near top-dead-centre. This analysis defined that at the end of compression stroke, engine model with toroidal shape piston give 34.8% improvement in term of swirl ratio and 7% improvement of tumble ratio value compared to original piston bowl shapes.

Keywords: Computational fluid dynamics, Swirl, Tumble, Cold flow, Piston bowl.

1. Introduction

In the development of automotive industry, internal combustion (IC) engine has been applied as dominant power plant in vehicles since their introduction even before a century ago. In the application of internal combustion engine in passenger

Nomenclatures

$I_{.sa}$	Moment of inertia of fluid mass about swirl axis, kg/m^2
$I_{.ta}$	Moment of inertia of fluid mass about tumble axis, kg/m^2
k	Turbulent kinetic energy, m^2/s^2
$L_{.sa}$	Magnitude of fluid angular momentum with respect to swirl axis, kg.m^2/s
$L_{.ta}$	Magnitude of fluid angular momentum with respect to tumble axis, kg.m^2/s
N	Engine operating speed, rpm
R_s	Swirl ratio, dimensionless
R_t	Tumble ratio, dimensionless

Greek Symbols

ω_s	Angular velocity of rotating flow with respect to swirl axis, rad/s

Abbreviations

BDC	Bottom Dead Centre
CFD	Computational Fluid Dynamics
IC	Internal Combustion
TDC	Top Dead Centre
CAD	Crank Angle Degree

vehicles, passengers continue to demand for improvement of engine system. As the improvement of engine is under significant pressure, researchers continue to pursue for different methodologies in order to accomplish engine analysis by means of low cost and obtaining good results. In this continuous approach for analysis method, Computational Fluid Dynamics (CFD) analysis has emerged from years ago as a new analysis tool in the understanding of complex fluid dynamics and chemical reaction occurred inside the engine throughout the cycles. Besides, computational simulation is also one of the powerful tools in design process as the flexibility of CFD simulation reduces the duration for model development [1, 2].

Proven significant advantages from applying CFD simulation have caused the simulation to become one of the crucial methods in analysis of engine system. Compared to analytical, experimental or lower multidimensional computational method, CFD allow designers to simulate and visualize the complex fluid dynamics with lower cost and lower analysis duration, providing that the simulation fulfil the optimized setup [3]. Example of experimental method available for engine flow analysis and charge motion study is the Flow Bench test. Although Flow Bench test is widely used to quantify the flow performance of engine, it is not efficient to be used alone for design of engine because it does not provide the designer with detail insight of the phenomenon occurs inside engine cylinder [4]. For analysis using lower multidimensional computational method, this method is also known as combination of simplified fluid dynamics simulation with thermodynamics data from experiments. Lower multidimensional simulation is a simulation computed with lower dimensionality which reduces the number of variables under consideration, thus reducing the complexity of the analysis. The application of lower multidimensional simulation such as 2-dimensional simulation is limited to the facts that simulation is only accurate if accompanied

with accurate data from experiment and correct assumption in the simplification process [5, 6].

Payri et al. [7] had carried out the CFD simulation on a single-cylinder Diesel engine for intake and compression stroke with different chambers. In the analysis the engine model does not include the exhaust port as it does not open during the intake and compression stroke. In the work by Payri et al. [7], the swirl ratio value is obtained from different points in the engine. Based on the result that the graph trends of swirl ratio at all location are almost the same, the swirl ratio for engine with different piston bowl configurations is compared at a chosen point inside the engine cylinder. Wu and Perng [8] performed the numerical analysis to investigate in-cylinder flow motion inside engine. However, the piston shape is relatively simple compared to the pistons used in the cars nowadays. Dinler and Yucel [9] performed CFD simulation for both flow and combustion in spark-ignition engine with a central spark plug. Standard k-epsilon turbulence model is utilized for the fluid flow while Eddy Break-up model is utilized for the combustion. However, the engine model use a flat piston which is also relatively simple compared to engine piston configuration nowadays.

In this study, effect of different piston bowl configurations on in-cylinder flow is investigated by using Cold Flow analysis. Modification is done on existing engine model to produce two new piston bowl shapes while retaining the geometry of other engine parts. This modification is based on the piston shapes that are commonly used nowadays. For the Cold Flow analysis, axisymmetric 3-dimensional model is used to compute the simulation. Standard k-epsilon turbulence model is utilized to investigate the in-cylinder flow condition which is quantified in term of swirl ratio and tumble ratio. Simulation is computed during intake stroke and compression stroke. By means of Cold Flow simulation, the pressure and temperature development in engine cylinder are also analysed without reaction from fuel injection or spark ignition. This provides the insight on real condition inside engine cylinder just before combustion.

Nowadays, direct-injection spark ignition system is getting the main attention due to its potential in significant fuel consumption reduction and power output. In direct-injection system, understanding on the flow characteristics is crucial to determine the efficiency of the system. Study on the flow characteristics of existing spark-ignition engine as conducted in this research allows for the opportunity to produce direct-injection gasoline engine based on modification of original engine.

2. Literature Review

2.1. Computational fluid dynamics of internal combustion engine

Computational Fluid Dynamics (CFD) analysis integrated the use of numerical methods, mathematical modelling and computational software to predict and visualize the qualitative and quantitative properties of fluid flows. CFD analysis is capable of solving various case study including single phase and multiphase condition, compressible or incompressible fluid flow, isothermal fluid flow, and also chemical reaction occurred in the flow. Encountering many phenomena involving fluid flow in everyday life, CFD has been continuously used in analysing ventilation, air conditioning, propulsion system, combustion of

automobile engine, and aerodynamics shape design. In the case of Internal Combustion (IC) engine, there are four methods available which differ from each other depending on the demanded results of users. These analysis mentioned are Port Flow analysis, Cold Flow analysis, In-Cylinder Combustion simulation and Full Cycle simulation.

For Port Flow analysis, the engine geometry is held frozen at critical crank angle of engine cycle, as selected by the users. This analysis holds major resemblance to the static analysis for any cases solved by CFD. For the simulation of combustion, CFD users are provided with the options of In-Cylinder Combustion simulation and Full Cycle simulation. However, in In-Cylinder Combustion simulation the analysis is computed during power stroke only. For Full Cycle simulation, CFD prediction from this analysis can provide full picture of the engine processes including modelling of air flow, injection of fuel, combustion and also formation of exhaust gases from the chemical reaction.

Meanwhile, Cold Flow simulation is categorized into transient simulation. In this analysis, full engine cycle can be simulated but without capturing the chemical reaction occurred. Cold Flow simulation can visualize the air flow throughout the cycle, capturing the induction of air, and predicting the formation of swirl, tumble and squish. Mixing of air with injected fuel can also be predicted but without the reaction. Since this simulation neglected those thermodynamics changes in the engine, the flow characterised in power stroke and exhaust stroke does not reflect reality [10].

Mass, momentum, energy and k-epsilon turbulence model without fuel injection and chemical reaction are described in the equation as below:

$$\frac{\partial \rho}{\partial t} + \nabla \left(\rho \underset{u}{\rightarrow}\right) = 0 \tag{1}$$

$$\frac{\partial \rho}{\partial t}\left(\rho \underset{u}{\rightarrow}\right) + \nabla \left(p \underset{u}{\rightarrow} \underset{u}{\rightarrow}\right) = \nabla P - \nabla\left(\frac{2}{3}\rho k\right) + \nabla \cdot \underset{\sigma}{\leftrightarrow} + \rho g \tag{2}$$

$$\frac{\partial \rho}{\partial t}(\rho I) + \nabla \left(p\, I \underset{u}{\rightarrow}\right) = -P\left(\nabla \cdot \underset{u}{\rightarrow}\right) - \nabla\left(\frac{2}{3}\rho k\right) + \nabla \cdot \underset{J}{\rightarrow} + \rho\varepsilon \tag{3}$$

$$\frac{\partial}{\partial t}(\rho k) + \nabla \left(p \underset{u}{\rightarrow} k\right) = -\frac{2}{3}\rho k \nabla \underset{u}{\rightarrow} + \underset{\sigma}{\leftrightarrow} \cdot \nabla \underset{u}{\rightarrow} + \nabla\left[\left(\frac{\mu}{Pr}\right)\nabla k\right] - \rho\varepsilon \tag{4}$$

$$\frac{\partial \rho}{\partial t}(\rho\varepsilon) + \nabla \left(p \underset{u}{\rightarrow} \varepsilon\right) = \left(\frac{2}{3}c_{z1} - c_{z3}\right)\rho\varepsilon \nabla \cdot \underset{u}{\rightarrow} + \nabla\left[\left(\frac{\mu}{Pr}\right)\nabla\varepsilon\right] + \frac{\varepsilon}{k}\left[c_{z1} \underset{\sigma}{\leftrightarrow} \cdot \nabla \underset{u}{\rightarrow} - c_{z2}\rho\varepsilon\right] \tag{5}$$

where ρ is density, $\bar{u}$ is velocity vector, P is pressure, σ is turbulent viscous stress tensor, I is specific internal energy and j is the heat flux vector [11].

2.2. Flow

Fluid motion within combustion chamber is important to be understood as it brings significant impact not only on the mixing of fuel and induced air, but as well as combustion speed and engine efficiency. On the other hand, together with good fuel injection system, efficient fuel-air mixture aid in improving the quality of emission from engine [12]. In investigation of fluid flow, common parameters discussed include turbulence, swirl, and tumble [13, 14].

2.2.1. Turbulence

In an engine, turbulence occurs as a result of high speed process involved in engine cycle. As an engine operating at high speed, air flows into and out of the engine in repeating cycle at relatively high speed; creating turbulent flow inside the cylinder. Turbulent flow in an engine is an important factor in determining the heat transfer, mixing of fuel with air, evaporation, and combustion that occur throughout the engine cycle. Designers demand for engine that can operate with high turbulence when the engine is near top-dead-centre (TDC). This condition is crucial because near TDC, ignition occurs and high turbulent flow allows for more rapid break up and spread the flame faster compared to low turbulence. Previous researches deemed that combustion chamber geometry is one of the important parameter to generate turbulence in engine which consecutively affecting the combustion. Other important factors that contribute to turbulence generation are the piston speed, inlet flow condition, and intake manifold design. The use of tumble flap, and valves with or without shroud, are also part of design ideas that are proven to influence the turbulent flow in engine [13, 15]. In relation to understand the turbulence by means of CFD simulation, turbulent kinetic energy is one of the useful descriptors that can be computed by the simulation.

2.2.2. Swirl

Swirl is defined as the rotational movement of air around the cylinder vertical axis. As one of the parameter used to quantify the in-cylinder fluid motion, swirl influent the heat transfer, combustion quality and emission in addition to affecting the mixing of air-fuel and combustion process [16]. Together with tumble, great intensity of these two parameters in induced flow during intake stroke will result in high turbulence in engine which can be retained during compression stroke [17, 18]. In reality, the nature of swirl phenomenon inside an engine is very difficult to be determined, yet to be predicted. Previously mentioned Flow Bench test is one of the methods frequently used to investigate the swirl in engine at steady state. In the measurement of swirl inside operating engine, swirl ratio is used to quantify swirl. Swirl ratio is defined as

$$R_s = {}^{\omega_s}/_{2\pi N} \tag{6}$$

where R_s is swirl ratio, ω_s is angular velocity of rotating flow at swirl axis, and N is engine operating speed [10]. In CFD simulation using ANSYS IC Engine, swirl ratio can be automatically generated by simulation by inserting the right command for swirl ratio. ANSYS IC Engine deduced the swirl ratio as

$$R_s = \frac{L_{\cdot sa}}{I_{\cdot sa}} \Big/ \frac{2\pi N}{60} \tag{7}$$

where $L_{\cdot sa}$ is magnitude of fluid angular momentum with respect to swirl axis, $I_{\cdot sa}$ is moment of inertia of fluid mass about swirl axis, and N is engine operating speed (revolution per minute) [10].

2.2.3. Tumble

When piston approaches top-dead-centre (TDC) at the end of compression stroke, mixture inside engine undergoes radially inward or transverse motion called squish. Tumble is the secondary rotational flow as a result of squish

motion when piston located nears TDC. Tumble is also defined as rotational flow occurred about circumferential axis near the piston bowl outer edge [13, 14, 19]. By means of experimental methods, tumble ratio is usually measured using steady flow rig at selected valve lift, but tumble ratio value are deemed specific on tumble rig design. Thus, different data of tumble ratio from experiment with different rigs cannot be compared directly [20]. In order to quantify the tumble in internal combustion engine, tumble ratio is the parameter discussed in this study.

In ANSYS IC Engine, tumble ratio is automatically computed under right simulation command. CFD simulation by ANSYS IC Engine computed tumble ratio as

$$R_t = \frac{L_{\cdot ta}}{I_{\cdot ta}} \Big/ \frac{2\pi N}{60} \tag{8}$$

where $L_{.ta}$ is magnitude of fluid angular momentum with respect to tumble axis, and $I_{.ta}$ is moment of inertia of fluid mass about tumble axis [10]. In addition to tumble ratio, ANSYS IC Engine introduce another parameter which is the cross tumble ratio which involve the computation of rotational flow at the axis perpendicular to tumble axis which also known as cross tumble axis.

3.Methodology

3.1. Modelling of engine

The engine studied in this research is a pent-roof engine with two exhaust valve and two intake valve. The initial model used is the model taken from ANSYS tutorial which is then modified into two other models with different bowl configurations while retaining the geometry of other engine parts. The modification is based on the piston bowl shapes that are commonly used in automobile engine. The selection of piston bowl shapes are also based on the fact that the fabrication process for producing real engine should not be complicated [20]. Computational model of engine for analysis include the intake valve, exhaust valve, cylinder and piston bowl. The initial engine model is symmetrical which is becoming the factor of having only half of the computational model. Analysis of engine model as symmetry will reduce the number of grid cell as well as reduction in computational time.

Shapes of the piston modified from the initial model are the common shapes of piston bowl used in engine cylinder. In order to properly analyse the effect of different geometrical properties of the bowls on in-cylinder flow, piston bowl depth and bowl diameter was held constant. Piston A represents the original bowl from the ANSYS tutorial model. Piston B has similar piston bowl shape as piston A except for higher throat diameter compared to piston A. For piston C, the bowl diameter and throat diameter is the same as piston A but it is modified into toroidal piston with centre pit. Figure 1 shows the initial engine model taken from ANSYS tutorial and Fig. 2 represents the three piston bowls shape that are analysed. The engine specifications for Cold Flow analysis are shown in Table 1.

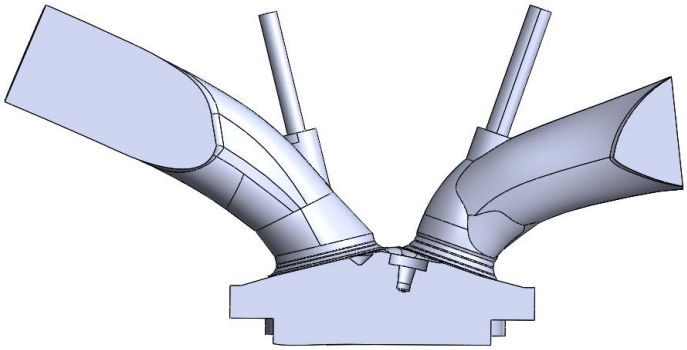

Fig. 1. ANSYS tutorial model [10].

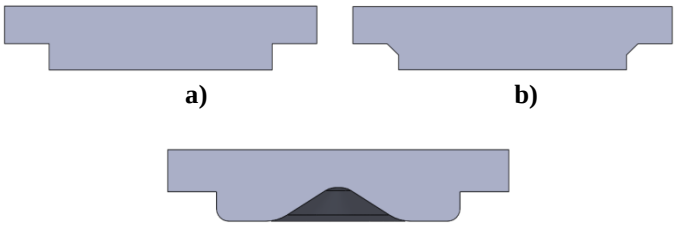

Fig. 2. Piston bowl shapes used in the analysis, a) Piston A, b) Piston B and c) Piston C.

Table 1. Engine specifications.

Parameter	Value
Connecting rod length (mm)	130
Crank radius (mm)	44
Piston offset (mm)	0
Engine speed (rpm)	3000
Minimum Lift (mm)	0.1
Bore (mm)	84
Stroke (mm)	88
Clearance Volume ($mm^{3)}$	47,290
Compression Ratio	6:1

These parameter values were taken from actual natural aspirated 1.6-liter engine which have high resemblance with the geometry of the initial model. The valve lift and piston motion profile are also based on that engine. All the parameters mentioned are the values that needed to be inserted at preliminary stage of Cold Flow simulation before inserting the engine model.

3.2. Decomposition and meshing

In order to accurately visualize the engine process as a transient simulation, the engine model was decomposed into different zone. This provides better control on

the mesh of model. In ANSYS Meshing, the decomposed zone is indicated by different label of the parts as shown in Fig. 3 and listed in Table 2.

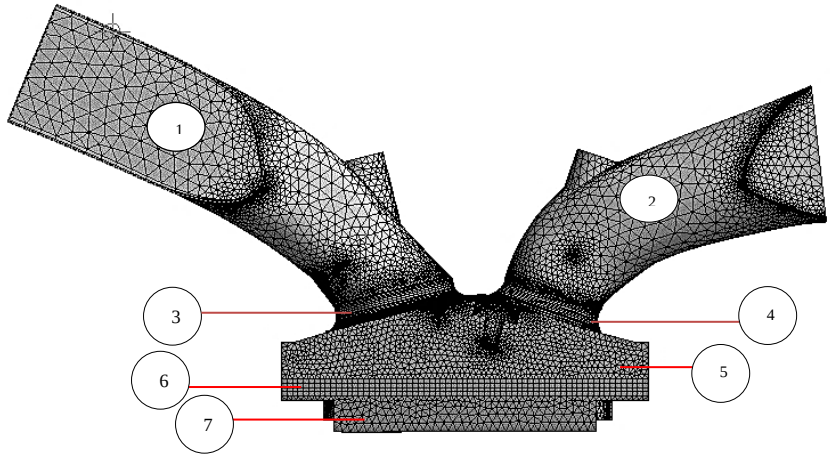

Fig. 3. Decomposition and meshing of model.

Table 2. Decomposed zones.

Zone No.	Decomposed Zone
1	Intake port
2	Exhaust port
3	Intake valve seat
4	Exhaust valve seat
5	Cylinder upper chamber
6	Cylinder layer
7	Piston

In ANSYS Meshing, model was decomposed into different regions which were mainly intake port, exhaust port, valves seat, and combustion chamber. From Fig. 3, it can be observed that different zones of the engine have different quality and different shape of grid cell. The grid cell is especially finer at region of cylinder combustion chamber and at the valve seat. For intake port and exhaust port, the grid is coarser than the other parts because this region is only static throughout engine cycle. At the valve seat, finer mesh cell is crucial to properly visualize the opening and the closing of valve, which in this study is only focused on intake valve opening and closing for induction of air into combustion chamber. During intake stroke and compression stroke, piston bowl will move along the stroke line from TDC to BDC and the other way round to complete the cycle. This is the reason why the combustion chamber was also separated into different zones as piston bowl is the only moving part while region near cylinder head is static. For more accurate analysis, moving zones were meshed with hexahedral cell, while static zones are meshed with tetrahedral cell to reduce computational time. The minimum number of mesh cell for respective model that can provide users with correct results is obtained by grid independence test.

3.3. Grid independence test

Grid independence test is done in order to find the minimum number of mesh cell that can give good result from the simulation. It is important to determine the right total number of mesh cell to ensure that it is neither too low until causing high deviation from the right result, nor too high that can cause long computational time. Figure 4 shows the grid independence test computed for original piston where result is compared in term of turbulent kinetic energy for six different number of mesh cell ranging from 580,000 to 900,000.

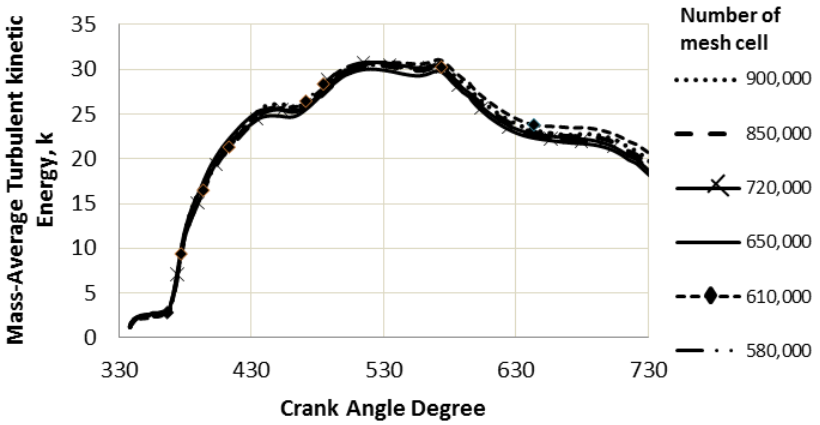

Fig. 4. Grid independence test for turbulent kinetic energy.

From Fig. 4, it can be observed that turbulent kinetic energy profile is very close to each other even at significance difference in number of mesh cell. At around 460 CAD, turbulent kinetic energy computed for engine with 580,000 and 610,000 mesh cells has a deviation of around 4% compared to the other four models with different mesh number. Another comparison is discussed by comparing the results of swirl ratio for engine model with different number of mesh cell as shown in Fig. 5.

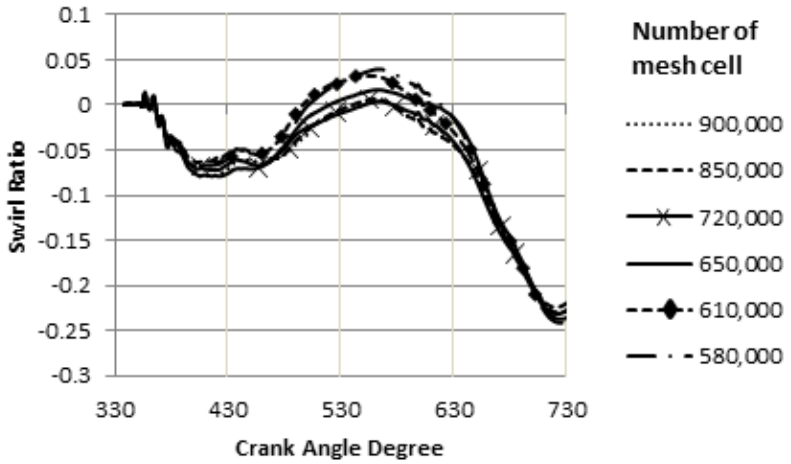

Fig. 5. Grid independence test for swirl ratio.

From Fig. 5, swirl ratio computed by Cold Flow simulation shows significant differences on the data for different number of mesh cell used. For 580,000, 610,000 and 650,000 of mesh cells used, results computed shows that the swirl ratio for these two models is closed to each other. When the mesh cell number is increased by hundred thousand, it can be observed that the deviation of swirl ratio values is large that is around 30 - 40%. For engine model with 720,000 mesh cells, swirl ratio profile obtained is closed to the model with 850,000 and 900,000 mesh cells. With 2 - 4% differences of computed value for the three mesh cell numbers, it is decided that number of grid cells used for all simulation is 720,000.

In this Cold Flow simulation, analysis only involved intake stroke and compression stroke. Thus, simulation is computed from around 5° before the opening of intake valve while exhaust valve is completely shut off throughout the simulation. Mass flow rate of induced air at the inlet port is set as 0.0103 kg/s and the inlet initial pressure is inserted as 98,900Pa. This initial condition is obtained from real engine model that has geometrical properties close to the initial computational model [21]. In this computation of Cold Flow simulation, analysis on engine is set as Standard k-epsilon model with Enhanced Wall Treatment utilized for wall treatment scheme. Enhanced Wall Treatment is a near-wall modelling approach that combines two-layer model with enhanced wall function. For enhanced wall function, this function composed of the blend of laminar wall law with turbulent wall law. Meanwhile, as an integral part of the enhanced wall treatment, two-layer model is used to specify turbulent viscosity and ε for the mesh layer at the wall. In the application of Enhanced Wall Treatment, this treatment is similar to standard two-layer model if the mesh layer at the wall is fine enough to resolve laminar sublayer which is usually $y^+ \approx 1$ [22]. PISO scheme is used along Green-Gauss Node Based for gradient and PRESTO! for pressure. To obtain more accurate results, second order upwind is set to solve for density, momentum and turbulent kinetic energy.

This study presents engine analysis starting from 330 CAD where at this crank angle, the opening of intake overlapped with closing of exhaust valve. Assuming that the remains of exhaust gases do not influence condition inside cylinder chamber, exhaust valve is completely close from 330 CAD until 720 CAD. Figure 6 shows the valves lift throughout the engine cycle where the opening and closing of both exhaust valve and intake valve can be properly observed.

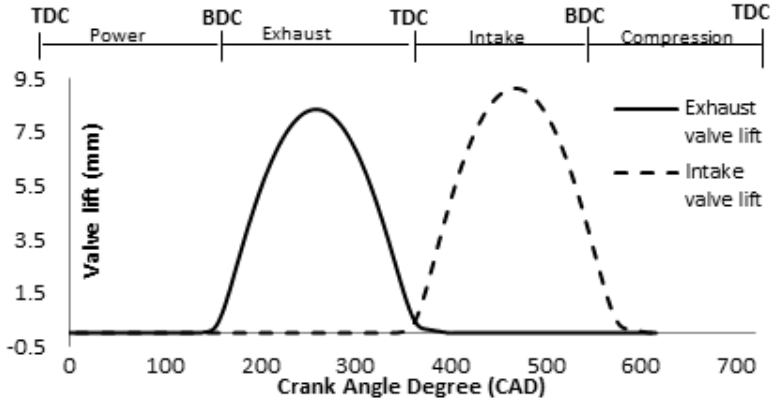

Fig. 6. Valves lift profile.

4. Results and Discussion

In order to quantify the flow in engine, swirl ratio is one of the parameters that are analysed in this study. Figure 7 shows the swirl ratio profile computed from 330 CAD to 720 CAD.

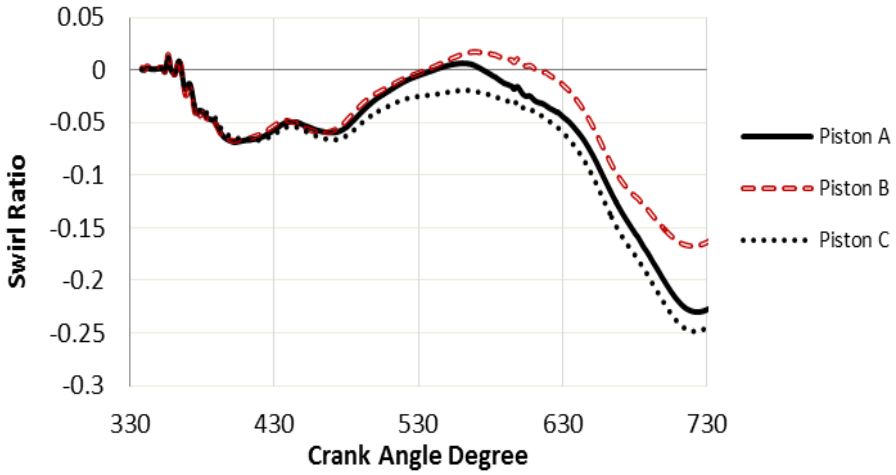

Fig. 7. Swirl ratio vs crank angle degree for different piston bowl geometries.

From Fig. 7, it can be observed that there is little fluctuation of swirl ratio value from 330 CAD to 380 CAD. This is predicted because during this interval, the intake valve opening is very small, thus forming high velocity intake air jet around valve opening. This is shown as in Fig. 8(a), where conical jet is formed around the intake valve; entering the cylinder.

From 330 CAD until 450 CAD where piston move from TDC to the middle of intake stroke, the swirl ratio value for piston A, B and C are very close to each other, indicating that piston bowls configuration does not affect the swirl formation during this interval. From the middle of intake stroke to BDC (450 CAD to 540 CAD) where intake valve start to close again, there are deviations of swirl ratio value for piston A, B and C. At around 565 CAD which is at the earlier stage of compression stroke, the swirl ratio value peaked for all three models. Figure 9 shows the velocity vector obtained at cross-sectioned plane 5mm above the piston at early of compression stroke. It can be observed from Fig. 9 that there are formations of vortex in the middle of cylinder and at the peripheral of cylinder near exhaust valve.

Piston C which have wide throat diameter give 23% decrement of swirl ratio compared to initial piston geometry which is Piston A. Meanwhile, modifying the piston into toroidal shape which is piston B has increased the swirl ratio value at 565 CAD by 7%. From 565 CAD to 720 CAD, swirl ratio values in all pistons undergo rapid decrement with similar trend. At the end of compression stroke, swirl ratio value in Piston B is around -0.17 which is 34.8% larger that piston A while Piston C have swirl ratio value which is 8.7% lower than piston A.

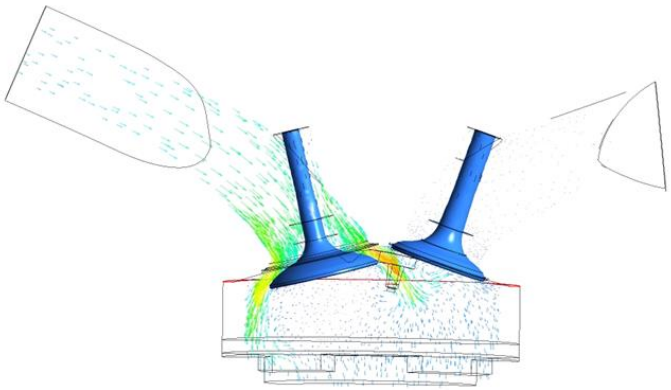

(a) 380 CAD

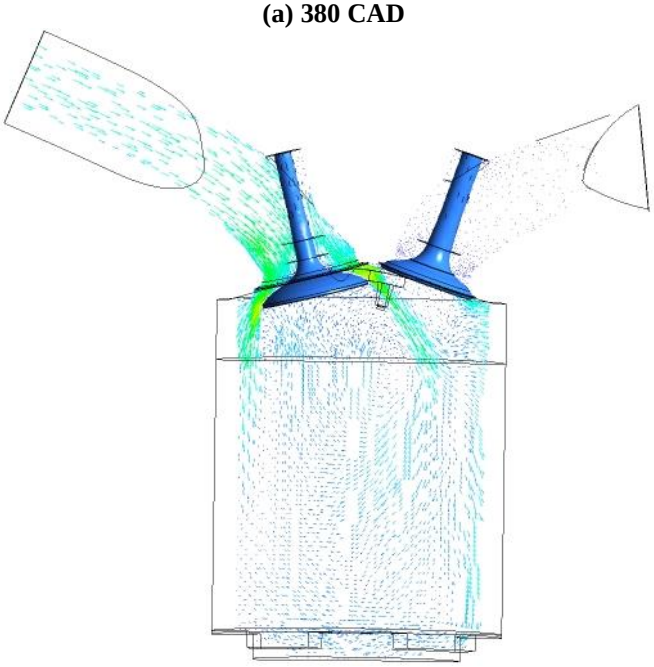

(b) 530 CAD

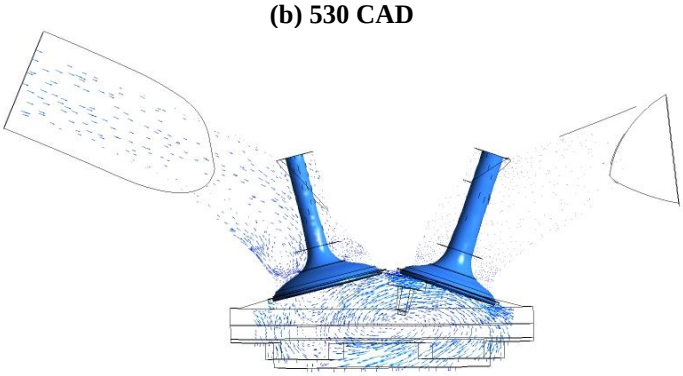

(c) 720 CAD

Fig. 8. Velocity vector at different crank angle degree, a) 380CAD, b) 530 CAD and c) 720 CAD

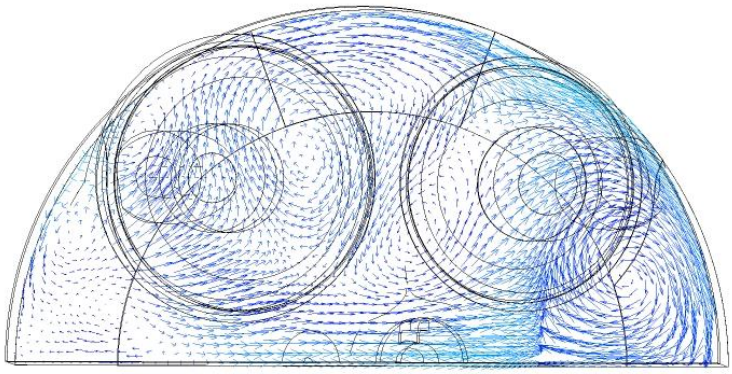

Fig. 9. Velocity vector at cross-sectioned plane 5 mm above the cylinder at 565 CAD.

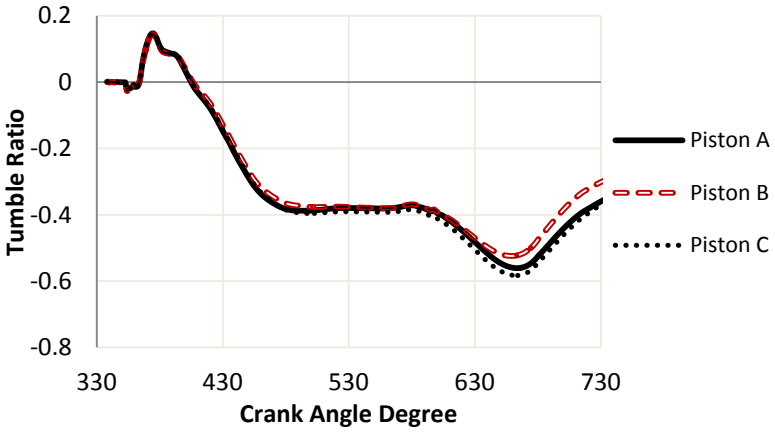

Fig. 10. Tumble ratio vs crank angle degree for different piston bowl geometries.

Tumble ratio is computed with respect to x-axis as shown in Fig. 10. From tumble ratio data for all piston shapes, it can be observed that there is small fluctuation from 330 CAD to 365 CAD before there is sudden increment from 365 CAD to 380 CAD. From 380 CAD to 450 CAD which is the opening of intake valve, tumble ratio decreases rapidly before approaching constant throughout the closing of intake valve (480 CAD to 580 CAD). At the earlier stage until the middle of compression stroke (580 CAD to 670 CAD), tumble ratio continue to decrease again before starting to have rapid increment when piston approaching TDC from middle of compression. Similar to swirl ratio, the effect of piston bowl shape on tumble ratio does not significantly take place during intake stroke. It can be observed from Fig. 10 that along intake stroke, the tumble ratio value for all pistons does deviate from each other, but the deviation is very small which is only around 0.8%. However, there are significant deviation of value in both tumble ratio and swirl ratio during compression stroke. At the end of compression stroke, Piston B which has toroidal shape is computed with highest tumble ratio value compared to other pistons which is -0.3. Meanwhile, piston C with highest throat diameter is computed with lowest tumble ratio at the end of compression stroke which is -0.38.

Cross tumble ratio is computed with respect to y-axis in order to provide better insight on the flow inside combustion chamber. Cross tumble ratio for intake and compression stroke are computed in Fig. 11.

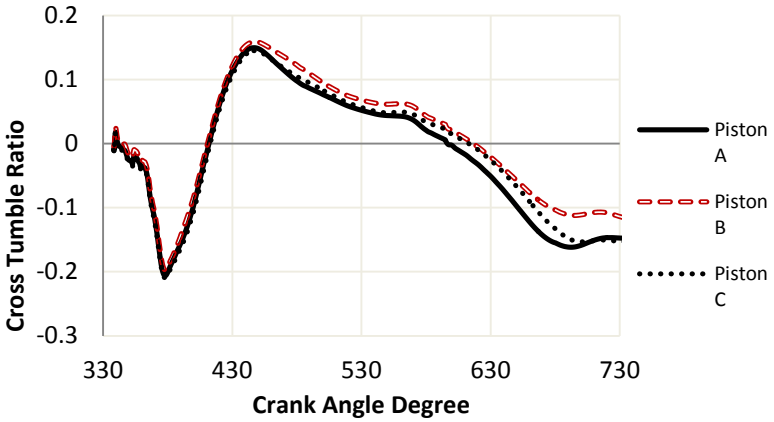

Fig. 11. Cross tumble ratio vs. crank angle degree for different piston bowl geometries.

Similar to the change in swirl ratio and tumble ratio, at earlier stage of the simulation (330 CAD to 365 CAD), there is small fluctuation of cross tumble ratio value. From 365 CAD to 380 CAD, there is steep decrement in the value of cross tumble ratio. This is because at earlier part of intake stroke, piston position is at TDC. When air is induced into engine cylinder, due to the direction of intake flow, tumble formation is high around x-axis which is in the direction of air flow while tumble around y-axis is low as it is perpendicular to the direction of induced air. When the opening of intake valve continues to increase from 380 CAD to 450 CAD, cross tumble ratio also increased rapidly. In the analysis of piston bowl effect on cross tumble ratio, in can be observed that for this respective engine model, the shape of piston bowl influence the cross tumble ratio starting from middle of intake stroke all the way to the end of compression stroke. From 450 CAD to 650 CAD, different piston bowl shapes are computed with different cross tumble ratio values with 4 - 6% differences with each other. At the end of compression stroke, the difference in term of cross tumble ratio for Piston B compared to other pistons is very significant which is around 17%.

Turbulent kinetic energy is another parameter discussed to properly understand the flow criteria in the engine cylinder. Figure 12 shows the turbulent kinetic energy profile throughout the intake stroke and compression stroke.

It can be observed that turbulent kinetic energy increased as piston move from TDC to BDC during intake stroke. From Fig. 8, at the early of induction, the turbulent flow inside engine is highly a non-homogenous. Recirculation is shown by the velocity vortex at the zones where the intake air jets collide. As the cylinder volume increased, the turbulent flow inside combustion chamber which is started by the induction of air continues to develop. From Fig. 8(b), turbulence is clearly more homogenous inside the cylinder even though there is small area of strong turbulence near the intake valve. This fact is further approved by the computational data where Fig. 12 shows that from 540 CAD to 720 CAD (BDC to TDC), turbulent kinetic

energy decrease again along the compression stroke. Decrease in term of cylinder volume during compression stroke caused the turbulent to settle down inside the cylinder. Along intake stroke and compression stroke, the piston bowl shapes do not give significant influence on turbulence as turbulent kinetic energy computed for all pistons give relatively similar values throughout the simulation.

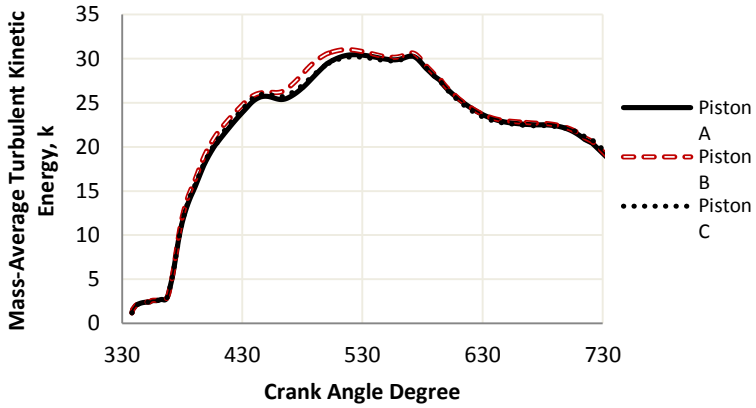

Fig. 12. Turbulent kinetic energy vs. crank angle degree for different piston bowl geometries.

Figure 13 below shows the velocity vector for all three pistons at 720 CAD. In all engine cylinders, vortexes are formed at the central of the engine cylinder. As shown in Fig. 8, at early of induction, flow velocity is higher particularly at the middle of cylinder and cylinder wall where the intake air jet impinges. Approaching end of intake stroke, the turbulent become more homogenous inside cylinder. When engine advanced into compression stroke, decrease in the cylinder volume and the effect of squish and tumble caused the development of the vortex.

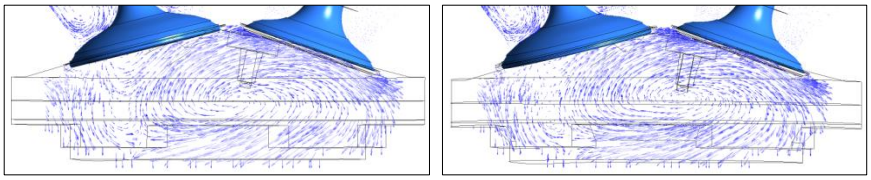

(a) Original piston **(b) Widethroat piston**

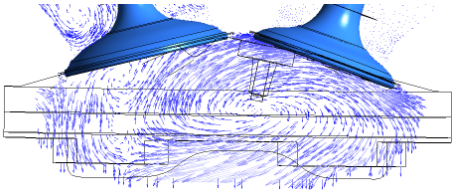

(c) Toroidal piston

Fig. 13. Velocity vector in a) original piston, b) wide throat piston and c) toroidal piston at 720 CAD.

Cylinder pressure and cylinder temperature are another parameters discussed in Cold Flow simulation. To properly observe the pressure and temperature development without reaction in engine cylinder, the simulation is extended to 830 CAD which is the middle of power stroke. Data of absolute pressure versus crank angle degree is plotted as in Fig. 14.

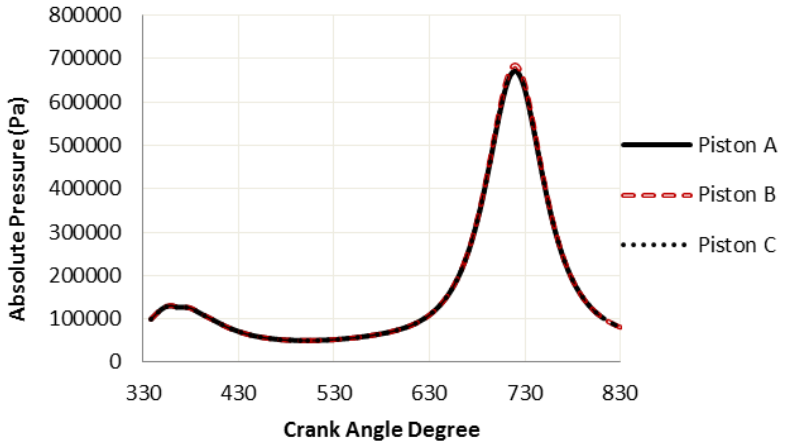

Fig. 14. Absolute pressure vs. crank angle degree.

From 330 CAD to 380 CAD, the absolute pressure undergoes slight increase. This is predicted because it is assumed in this simulation that at 330 CAD, engine is not operating before induction of air is introduced into the engine system. Cold Flow analysis computed the absolute pressure profile where at the end of compression stroke (TDC), absolute pressure reached the peak at 690kPa. It can be observed that piston bowl configurations do not influence pressure development inside engine cylinder. There is small difference of peak pressure for Piston B compared to other pistons. This is because of modifying of piston geometry which causes Piston B to have slightly higher compression ratio compared to Piston A and C.

Cylinder temperature development from intake stroke until the middle of power stroke is as plotted in Fig. 15.

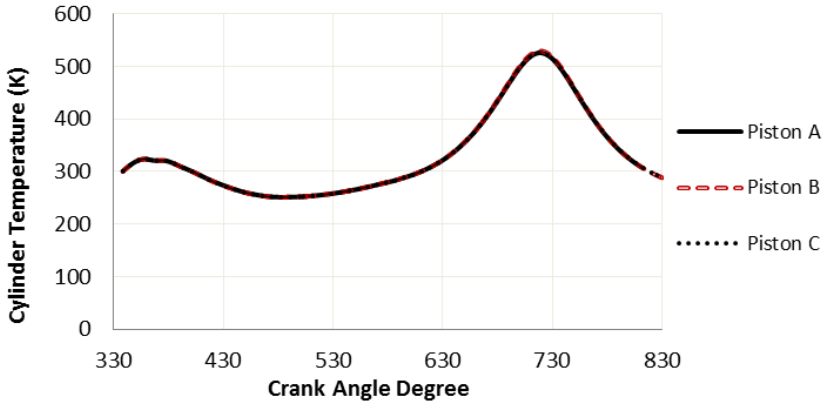

Fig. 15. Cylinder temperature vs. crank angle degree.

At the earlier part of the simulation, cylinder temperature undergoes slight increase before drop to slightly lower value starting from 380 CAD. Initial temperature assigned to the combustion cylinder is 300K, which then dropped due to the induction of air into the system. As intake air temperature is assigned to surrounding temperature, the induction of air causes the cooling inside combustion chamber. At 720 CAD, cylinder temperature reaches the peak value at 535K. Cylinder temperature profile computed in Cold Flow simulation is relatively similar to any cylinder temperature trend that has been obtained from any other analysis method.

5. Conclusions

Cold Flow simulation is used to analyse in-cylinder flow properties for a pent-roof engine throughout intake stroke and compression stroke. Resulting flow conditions are compared between three engines that have different piston bowl configurations. From the simulation, it can be concluded that piston bowl shapes do not give significant influence on swirl and tumble during intake stroke. The differences inflicted on the flow properties which are the swirl ratio, tumble ratio and cross tumble ratio due to piston bowl geometries is only around 2 - 7% during intake stroke. However, during compression stroke, the effect of piston bowl configurations on flow condition is clearly significant. As piston approaching top-dead-centre, while piston which is modified to have wider throat diameter caused decrement of swirl ratio, tumble ratio and cross tumble ratio, piston modified into toroidal shape enhance the swirl and tumble inside cylinder. As flow condition inside engine cylinder influence the quality of combustion and mixing of air with fuel, piston bowl configuration is proved to be one of the important parameters in producing efficient engine. CFD simulation done in this engine study shows that piston bowl geometry does not influence the turbulence of flow. Turbulent kinetic energy which is the parameter used to quantify the turbulence is analysed and result bring forward the fact that turbulence developed during intake stroke and drop during compression stroke. Increment in the cylinder volume enhances the formation of turbulent flow while decrement in cylinder volume caused the turbulent flow to become homogenous and decrease in value along compression stroke. CFD simulation on engine by means of Cold Flow analysis also provides insight on cylinder pressure and temperature development. In this study, pressure and temperature plotted for analysed engine are relatively the same with other engines in term of trends. In this study, the peak pressure and peak temperature computed are 690kPa and 535K which is reasonably correct compared to other similar engine system in study by other researchers. Cold Flow simulation proved to give advantages in the analysis of engine. Years ago, Cold Flow analysis focused more on the Diesel engine as it operates on direct-injection system, thus the analysis of flow is critical. Nowadays, development of direct-injection gasoline engine is getting greater attention. This research on-spark ignition engine proves that different piston bowl configurations also bring significant effect on the flow even at low compression ratio of Gasoline engine compared to Diesel engine. Insight provided by this Cold Flow analysis allows researcher to do minor modification on existing Port Fuel Injection engine to operate as Gasoline Direct-injection engine.

Acknowledgements

The authors acknowledge the financial support from Universiti Teknologi Malaysia (UTM) and Ministry of Higher Education Malaysia (MOHE) under the FRGS grant R.J130000.7809.4F174.

References

1. Abdalla, M.O.; and Nagarajan, T. (2015). A computational study of the actuation speed of the hydraulic cylinder under different ports' sizes and configurations. *Journal of Engineering Science and Technology* (*JESTEC*), 10(2), 160-173.
2. Aroussi, A.; Lad, N.; Muhamad Said, M.F.; Adebayo, D.; and Al-Atabi, M. (2010). The interaction of a cold atomised spray with a circular cylinder. *Journal of Engineering Science and Technology* (*JESTEC*), 5(3), 361-372.
3. Pathak, Y.R.; Deore, K.D.; and Maharu, P.V. (2014). In cylinder cold flow CFD simulation of IC engine using hybrid approach. *International Journal of Research in Engineering and Technology*, 3(8), 16-21.
4. Balakrishnan, V.K.; Morton, S.; Radavich, P.; Sivagaminathan, N.; and Gopalakrishnan, N. (2010). Air flow and charge motion study of engine intake port. *37th National and 4th International Conference on Fluid Mechanics and Fluid Power*. Chennai, India, 1-9.
5. Chiodi, M. (2011). *An innovative 3D-CFD-approach towards virtual development of internal combustion engine* (1st ed.). Germany: Vieweg+Teubner Verlag.
6. Paul, B.; and Ganesan, V. (2010) Flow field development in a direct injection diesel engine with different manifolds. *International Journal of Engineering, Science and Technology*, 2(1), 80-91.
7. Payri, F.; Benajes, J.; Margot, X.; and Gil, A. (2004). CFD modelling of the in-cylinder flow in direct-injection diesel engines. *Computers and Fluids*, 33(8), 995-1021.
8. Wu, H.W; and Perng, S.W. (2004). Numerical analysis of thermal turbulent flow in the bowl-in-piston combustion chamber of a motored engine. *International Journal of Thermal Sciences*, 43(10), 1011-1023.
9. Dinler, N.; and Yucel, N. (2007). Numerical simulation of flow and combustion in an axisymmetric internal combustion engine. *International Scholarly and Scientific Research & Innovation*, 1(12), 692-697.
10. ANSYS, Inc. (2013). Internal combustion engine in workbench. Retrieved March 10, 2015, from http://www.ansys.com.
11. Kurniawan, W.H; Abdullah, S.; and Shamsudeen, A. (2007). A computational fluid dynamics study of cold-flow analysis for mixture preparation in a motored four-stroke direct injection engine. *Journal of Applied Sciences*, 7(19). 2710-2724.
12. Pulkrabek, W.W. (2003). *Engineering fundamentals of internal combustion engine* (2nd ed.). New Jersey: Prentice Hall.
13. Heywood, J.B. (1988). *Internal combustion engine fundamentals* (1st ed.). United States: McGraw-Hill, Inc.

14. Han, S.B.; Chung, Y.J.; and Lee, S. (1995). Effect of engine variables on the turbulent flow of a spark ignition engine. *Journal of Mechanical Science and Technology*, 9(4), 492-501.
15. Bharathi, V.V.P; and Prasanthi, G. (2013). The Influence of air swirl on combustion and emissions in a diesel engine. *International Journal of Research in Mechanical Engineering & Technology*, 3(2), 14-16.
16. Priscilla; and Meena, P. (2013). A comprehensive study on in-cylinder IC engine due to swirl flow. *International Journal of Engineering Research & Technology*, 2(7), 1156-1161.
17. Barbouchi, Z.; and Bessrour, J. (2009). Turbulence study in the internal combustion engine. *Journal of Engineering and Technology Research*, 1(9), 194-202.
18. Pfeffer, T.; Bühler, P.; Meier, D.; and Hamdani, Z. (2002). Influence of intake tumble ratio on general combustion performance, flame speed and propagation at a formula one type high-speed research engine. *SAE 2002 World Congress (2002-01-0244)*. Detroit, Michigan.
19. Abianch, O.S.; Mirsalim, M.; and Sabet, A.S. (2009). Investigation of swirling and tumbling flow pattern of spark ignition engine. *The Journal of Engine Research*, 14(14), 27-34.
20. Muhamad Said, M.F.; Abdul Aziz, A.; Abdul Latiff, Z.; Mahmoudzadeh Andwari, A.; Mohamed Soid, S.N. (2014). Investigation of cylinder deactivation (CDA) strategies on part load conditions. *SAE Technical Paper* 2014-01-2549.
21. Zhao, F.; Lai, M.C.; and Harrington, D.L. (2000). *Automotive spark-ignited direct- injection gasoline engines*. Pergamon: Elsevier.
22. ANSYS, Inc. (2013). Fluent User's Guide. Retrieved May 26, 2014, from http://www.ansys.com.